

Agonist-dependent Endocytosis of γ -Aminobutyric Acid Type A (GABA_A) Receptors Revealed by a $\gamma 2(\text{R43Q})$ Epilepsy Mutation*

Received for publication, March 28, 2013, and in revised form, July 30, 2013. Published, JBC Papers in Press, August 9, 2013, DOI 10.1074/jbc.M113.470807

Severine Chaumont^{†‡§1}, Caroline André^{‡§5}, David Perrais^{¶||}, Eric Boué-Grabot^{**‡‡}, Antoine Taly^{§§}, and Maurice Garret^{†§2}

From the [†]Université Bordeaux, Institut de Neurosciences Cognitives et Intégratives d'Aquitaine (INICIA), UMR 5287, F-33000 Bordeaux, France, [§]CNRS, INICIA, UMR 5287, F-33000 Bordeaux, France, [¶]Université Bordeaux, Institute for Interdisciplinary Neuroscience (IINS), UMR 5297, F-33000 Bordeaux, France, ^{||}CNRS, IINS, UMR 5297, F-33000 Bordeaux, France, ^{**}Université Bordeaux, Institut des Maladies Neurodégénératives, UMR 5293, F-33000 Bordeaux, France, ^{‡‡}CNRS, Institut des Maladies Neurodégénératives, UMR 5293, F-33000 Bordeaux, France, and ^{§§}CNRS, UPR 9080, Institut de Biologie Physico-Chimique, 13 Rue Pierre et Marie Curie, 75005 Paris, France

Background: Modulation of GABA_A receptors trafficking is critical for controlling inhibitory neurotransmission.

Results: A point mutation or agonist application, both affecting the GABA_A receptor extracellular domain, has an effect on receptor endocytosis.

Conclusion: Endocytosis of GABA_A receptors is linked to agonist-induced conformational changes.

Significance: This represents one of the few reports demonstrating an influence of extracellular effectors on GABA_A receptor trafficking.

GABA -gated chloride channels (GABA_A Rs) trafficking is involved in the regulation of fast inhibitory transmission. Here, we took advantage of a $\gamma 2(\text{R43Q})$ subunit mutation linked to epilepsy in humans that considerably reduces the number of GABA_A Rs on the cell surface to better understand the trafficking of GABA_A Rs. Using recombinant expression in cultured rat hippocampal neurons and COS-7 cells, we showed that receptors containing $\gamma 2(\text{R43Q})$ were addressed to the cell membrane but underwent clathrin-mediated dynamin-dependent endocytosis. The $\gamma 2(\text{R43Q})$ -dependent endocytosis was reduced by GABA_A R antagonists. These data, in addition to a new homology model, suggested that a conformational change in the extracellular domain of $\gamma 2(\text{R43Q})$ -containing GABA_A Rs increased their internalization. This led us to show that endogenous and recombinant wild-type GABA_A R endocytosis in both cultured neurons and COS-7 cells can be amplified by their agonists. These findings revealed not only a direct relationship between endocytosis of GABA_A Rs and a genetic neurological disorder but also that trafficking of these receptors can be modulated by their agonist.

Inhibitory transmission relies greatly on ionotropic GABA_A receptors (GABA_A Rs)³ that are involved in many physiological

functions and are the target of several drugs in wide clinical use (1). GABA_A R trafficking is modulated by a number of different mechanisms, including surface targeting, mobility, and endocytosis. Moreover, studies in physiological and pathophysiological states have revealed that the number of GABA_A Rs on the cell membrane have a profound influence on GABA_A ergic neurotransmission (1–3). Inhibitory neurotransmission is also regulated by the exchange between surface and intracellular compartments via a constitutive clathrin-mediated dynamin-dependent endocytosis pathway (4–6). This constitutive internalization is modulated by intracellular mechanisms and is altered in pathological conditions (4, 6–9).

Epilepsies are complex syndromes with multiple causes and symptoms, but it is well established that alteration or modulation of GABA neurotransmission plays an important role in the disease and its treatment (10–15). Moreover, genetic evidence has revealed a direct link between epilepsy and GABA_A R dysfunction, including trafficking alteration, supporting the hypothesis that defects in GABA_A Rs lead to seizures (16–17). These mutations also offer an opportunity to obtain new insights into GABA_A R structure and function as well as clues to the role of these receptors in neurological disorders (14). For example, an R43Q mutation located in the $\gamma 2$ subunit N-terminal extracellular domain is linked to childhood absence epilepsy and febrile seizure (17); heterozygous mice harboring this mutation replicate the human clinical phenotype (16). Intensive research into this mutation (18–26) has led to controversial data on its effects on GABA_A ergic physiology suggesting that $\gamma 2(\text{R43Q})$ might modify the dynamics of subunit trafficking (27).

Here, we analyzed $\gamma 2(\text{R43Q})$ trafficking in cultured hippocampal neurons and COS-7 cells and revealed that receptors containing the $\gamma 2(\text{R43Q})$ subunit had a shorter residence time on the plasma membrane than their wild-type counterparts.

* This work was supported by CNRS, Université de Bordeaux, Conseil Régional Aquitaine, and Fédération de la Recherche sur le Cerveau.

¹ Present address: Institut de Génétique Fonctionnelle, Universités de Montpellier 1 and 2, UMR-5203 CNRS, 141 Rue de la Cardonille, 34094 Montpellier Cedex 5, France.

² To whom correspondence should be addressed: CNRS UMR 5287, Université de Bordeaux2, 146 Rue Leo Saignat, 33076 Bordeaux Cedex, France. Tel.: 33-557571686; Fax: 33-556901421; E-mail: maurice.garret@u-bordeaux2.fr.

³ The abbreviations used are: GABA_A R, GABA_A receptor; ERGIC, endoplasmic reticulum-Golgi intermediate compartment; MESNA, sodium 2-mercaptoethanesulfonate.

We also showed that endocytosis of the mutated receptor was clathrin- and dynamin-dependent. However, it was surprising that a mutation in the extracellular domain (bearing binding sites for agonists and modulators) could have an influence on internalization, believed to be controlled through the intracellular domain. Moreover, endocytosis of GABA_ARs triggered by agonist exposure remains to be fully assessed (11, 28–31). Then, by using both imaging and biochemical methods, further experiments revealed that agonist exposure triggered an increase of wild-type GABA_AR endocytosis, both on native and recombinant GABA_ARs.

EXPERIMENTAL PROCEDURES

Antibodies and Reagents—Antibodies were raised in rabbits against the $\alpha 1$ GABA_A subunit N terminus (Alomone Labs), the Myc tag (Upstate, Charlottesville, VA), membrin (1:1000; Synaptic Systems), calreticulin (1:500; Upstate Biotechnology, Inc.), or EEA1 (Sigma-Aldrich). Antibodies were raised in mice against the $\alpha 1$ intracellular loop (Neuromab) or the Myc tag (Roche Applied Science). Secondary antibodies were as follows: Alexa Fluor-568 goat anti-rabbit, Alexa Fluor-647 goat anti-rabbit, Alexa Fluor-488 goat anti-mouse (1:1000; Molecular Probes), and FITC-coupled anti-mouse antibody (1:200; Chemicon).

DNA Constructs— $\alpha 1$, $\beta 2$, $\beta 3$, and $\gamma 2S$ GABA_AR subunits were subcloned in the pcDNA3 vector (Invitrogen), using constructs that were available from previous studies (32, 33). The Myc epitope (MEQKLISEEDLNE, repeated 6 times) was inserted between amino acids 4 and 5 of the $\gamma 2$ subunit (22). As described previously, an insertion within this domain does not modify the functional properties of GABA- or glutamate-gated channels (32, 34–36). Point mutations were constructed using the QuikChange site-directed mutagenesis system (Stratagene). All constructs were verified by automatic dideoxy DNA sequencing (Genome Express, Meylan, France). Endoplasmic reticulum-Golgi intermediate compartment was revealed with ERGIC-GFP (37), kindly provided by Jochen Lang (Bordeaux, France).

Cell Culture and Transfection—COS-7 and HEK 293 cells were maintained in Dulbecco's modified Eagle's medium (Invitrogen) supplemented with 10% fetal calf serum (Eurobio). Embryonic hippocampal neurons were obtained from E18 rat embryos, as described earlier (22). COS-7 and HEK 293 cells were transfected using the FuGENE 6 reagent (Roche Applied Science), according to the manufacturer's specifications, with equal amounts of $\alpha 1$, β , and $\gamma 2$ subunit cDNAs (and GFP for electrophysiology experiments on HEK 293 cells) (0.3 μ g/well in 24-well plates). Cells were incubated with cDNAs for 24 h before analysis (22). Hippocampal neurons were transfected *in vitro* at 7–11 days, using the Lipofectamine 2000 reagent (Invitrogen) according to the manufacturer's specifications. The cells were analyzed 24–60 h after transfection (22).

Immunocytochemistry—For living cell surface labeling, COS-7 cells and hippocampal neurons were incubated with antibodies at room temperature for 20 min in Dulbecco's modified Eagle's medium or Neurobasal medium supplemented with 10 mM HEPES, respectively. Receptors on the surface were labeled with antibodies raised in rabbits against either the $\alpha 1$

GABA_A subunit N-terminal domain or the Myc tag. Sera were diluted 1:500 (anti- $\alpha 1$) or 1:200 (anti-Myc) in medium. After incubation, cells were washed quickly by dipping coverslips in medium and fixed for 10 min in phosphate-buffered saline (PBS) containing 4% sucrose and 4% paraformaldehyde preheated to 37 °C, washed in PBS, and blocked in 0.3% bovine serum albumin and 50 mM glycine (in PBS) for 15 min. Cells were washed in PBS containing 0.3% bovine serum albumin. After cell permeabilization using 0.3% Triton X-100, intracellular tagged $\gamma 2$ subunits were detected by incubating the cells with a mouse anti-Myc 9E10 antibody (1:1000; Roche Applied Science) for 2 h. Intracellular $\alpha 1$ subunits were detected with a mouse anti- $\alpha 1$ (1:1000). Polyclonal and monoclonal antibodies were detected using an Alexa Fluor-568-coupled anti-rabbit antibody and an Alexa Fluor-488-coupled anti-mouse antibody (1:1000), respectively. Endoplasmic reticulum and *cis*-Golgi staining were revealed with polyclonal anti-calreticulin (1:500) and anti-membrin (1:1000), respectively. The endoplasmic reticulum-Golgi intermediate compartment was revealed with ERGIC-GFP (37).

Internalization—Transfected neurons or COS cells were incubated in culture medium containing mouse monoclonal Myc antibody (1:200) at 37 °C for 30 min. The medium also contained GABA_AR agonists or antagonists as required. In the case of neurons, a mixture of inhibitors (6-cyano-7-nitroquinoxaline-2,3-dione (10 μ M), D-2-amino-5-phosphonovaleric acid (50 μ M), and tetrodotoxin (1 μ M)) was added, so as to prevent activity-dependent modulation of GABA_AR trafficking (7). This mixture was added 5 min before the labeling experiments and was present throughout, both in control experiments and in GABA_AR agonist/antagonist-treated neurons. Surface labeling was carried out at 20 °C using an anti-mouse secondary antibody coupled to Alexa Fluor-647 for 30 min (38); alternatively, labeled receptors remaining on the COS-7 cell surface were acid-washed for 2 min at 20 °C with culture medium adjusted at pH 2.5 (39, 40). Cells were then fixed using 4% paraformaldehyde in 4% sucrose and permeabilized in Triton X-100. Total protein content was assessed by incubating with a polyclonal antibody directed at the Myc tag. Internalized protein was then revealed by incubating with anti-mouse antibody coupled to Alexa Fluor-488 at room temperature for 1 h, whereas total protein was revealed using anti-rabbit antibody coupled to Alexa Fluor-568. For native $\alpha 1$ expressed in hippocampal neurons, cells were incubated in culture medium containing an antibody made in rabbits directed at the N-terminal domain (extracellular) of $\alpha 1$ (1:500) at 37 °C for 30 min. Surface labeling was carried as above using an anti-rabbit secondary antibody. Cells were then fixed and permeabilized as above. Total $\alpha 1$ subunit content was assessed by incubating with a mouse antibody directed at the Myc tag or at the native $\alpha 1$ at room temperature for 20 min. Internalized protein was then revealed by incubating cells with anti-mouse antibody coupled to Alexa Fluor-488 at room temperature for 1 h, whereas total protein was revealed using anti-rabbit antibody coupled to Alexa Fluor-568.

Quantitative Analysis of Fluorescence Signals—Fluorescence microscopy was performed using a Zeiss Axioplan 2 microscope, with a $\times 63$, 1.4 numerical aperture oil immersion lens.

$\gamma 2(R43Q)$ and GABA_AR Trafficking

Quantification of fluorescence signals and background subtraction were performed using ImageJ (National Institutes of Health). For each image acquired, background levels were determined using the surface and intracellular signals measured in neighboring non-transfected cells and subtracted from the values obtained in transfected cells. Numerical data are presented as mean \pm S.E., and statistical significance was assessed using one-way analysis of variance (Origin, Originlab Corp.) (significance level, $p < 0.05$). Confocal microscopy was performed using an upright Leica DMR TCS SPZ AOBS, with a $\times 63$, 1.4 numerical aperture Leica HPCL Fluotar oil objective. Colocalization was quantified using a plugin for ImageJ designed by F. Levet and C. Poujol (BIC (Bordeaux Imaging Center), Bordeaux, France). Briefly, two images, one containing GABA_AR subunit labeling and one containing the labeling for a cellular compartment, were thresholded in the same way. The plugin calculates the percentage of pixels containing $\gamma 2$ subunit labeling that also contain specific labeling for a cellular compartment. The percentage of colocalization was normalized for total $\gamma 2$ and $\gamma 2(R43Q)$ immunoreactivity, respectively. Analyses were performed in parallel cultures, blind to experimental conditions.

Quantification of surface clusters or intracellular punctate labeling, blind to experimental conditions, was performed using ImageJ (National Institutes of Health). Threshold was applied to the images, and the number as well as the area of surface clusters or internalized particles were measured using the particle analyzer module of ImageJ. For COS-7 cells, the whole cell was counted. For neurons, an area of 10- μm length along a dendrite was counted. For all experiments, total protein expression was assessed by antibody labeling after permeabilization of the cells and was measured for the same area to allow normalization of the values. To calculate fluorescence ratios, a stack was created for each cell in ImageJ with the image corresponding to the surface and total labeling. This allows us to draw the outline of the cell and measure the average surface and total fluorescence for the same area.

Biotinylation Assays—Biotinylation experiments were performed essentially as described previously (36, 38). COS-7 cells were transfected in 6-well plates (2 wells/condition) and were incubated 24 h post-transfection. Cells were then washed two times with PBS, pH 8.0, incubated with 1 mg/ml EZ-Link Sulfo-NHS-SS-Biotin (Pierce) in PBS for 30 min at 4 °C, washed three times with PBS, and scraped in lysis buffer containing 25 mM HEPES, 150 mM NaCl, 1% Triton X-100, and a mix of protease inhibitors (Roche Applied Science). After centrifugation, the supernatant was immunoprecipitated with 50 μl of Immopure immobilized streptavidin-beaded agarose overnight at 4 °C and washed extensively. Surface and total proteins were separated on SDS-PAGE and revealed by Western blotting using anti-Myc antibodies at a 1:1000 dilution. Quantification of Western blots was performed using ImageJ (National Institutes of Health) or with the Chemi Doc XRS+ under the control of the Image Lab software (Bio-Rad). To assess $\gamma 2$ internalization, plates were returned to 37 °C for 30 min after biotinylation to allow endocytosis. Cells were then exposed to 50 mM MESNA, which cleaved biotin from proteins remaining on the surface. A sample was kept at 4 °C (instead of 37 °C) to

control to ensure that the cleavage with MESNA was complete. Samples were analyzed by Western blot as above.

Electrophoretic and Western Blot Analyses—COS-7 cells were homogenized in buffer containing 20 mM HEPES, 0.15 mM EDTA, and 10 mM KCl, pH 8, supplemented with a mixture of protease inhibitors (Roche Applied Science). The buffer was then adjusted to 12% sucrose, and after four more strokes, the cells were centrifuged at 2000 rpm for 3 min to remove genomic DNA. The supernatant was centrifuged at 15,000 rpm for 30 min. The pellet was recovered, and cell membranes were solubilized with 15 strokes in a buffer containing 20 mM Tris-HCl, 0.15 mM EDTA, 150 mM NaCl, 2% Triton X-100, and 0.5% deoxycholate, pH 8, supplemented with a mixture of protease inhibitors, and then incubated for 45 min. The sample was centrifuged for 45 min at 15,000 rpm. The supernatant was supplemented with loading buffer and analyzed as described (22).

Electrophysiology—Brightly fluorescent isolated HEK 293 cells were selected for recording. Cells were bathed in a solution containing 150 mM NaCl, 2 mM KCl, 2 mM MgCl₂, 2 mM CaCl₂, 10 mM glucose, 10 mM HEPES, equilibrated to pH 7.4 with NaOH. Cells were recorded in whole cell mode and placed under the flow of a theta tube pulled to a final opening of ~ 100 μm mounted on a piezoelectric translator (Physik Instrumente). Currents were evoked by applications of 100 μM GABA for 5 s every minute at -60 mV and recorded at a sampling frequency of 2 kHz by an EPC10 amplifier (HEKA). GABA was exchanged for gabazine (100 μM) and applied to the cell after 3 min, necessary for complete exchange. Thereafter, the medium was exchanged again for GABA, and we observed complete recovery of the response to the agonist. Data were analyzed with Igor 5 (Wavemetrics).

Model Building—The sequences of the human $\alpha 1$, $\beta 2$, and $\gamma 2$ GABA receptor subunits were retrieved from the Ligand Gated Ion Channel database (41). The model of the $\alpha 1\beta 2\gamma 2$ receptor was constructed by homology modeling using the structure of the glutamate-gated chloride channel as a template (Protein Data Bank code 3RIF) (42) and sequences alignments obtained with T-coffee (43). Homology modeling was performed with Modeler version 9.5 (44) using default settings. 100 models were prepared, and the best model according to the Discrete Optimized Protein Energy function (DOPE) was selected. Figures were prepared with PyMOL (77).

RESULTS

$\gamma 2(R43Q)$ Displays Increased Clathrin-mediated and Dynamin-dependent Endocytosis—To analyze the impact of the R43Q substitution on intracellular trafficking, the colocalization of wild-type or mutated $\gamma 2$ with markers of intracellular compartments was assessed in transfected, cultured hippocampal neurons (Fig. 1, A and B). Increased retention in the endoplasmic reticulum (CaR colocalization: $38.3 \pm 2.5\%$ for $\gamma 2(R43Q)$ -containing subunits *versus* $26.7 \pm 2.3\%$ for wild-type receptors, $n = 31$ and 27, respectively; $p < 0.005$) confirmed previous findings in heterologous cells (HEK293 (24)). However, importantly, $\gamma 2(R43Q)$ colocalization with Golgi apparatus markers did not differ significantly from that of the wild-type subunit, showing that the mutated subunit was also present on the route to the cell membrane (membrin: $19.3 \pm 2.4\%$ for the wild-type *versus*

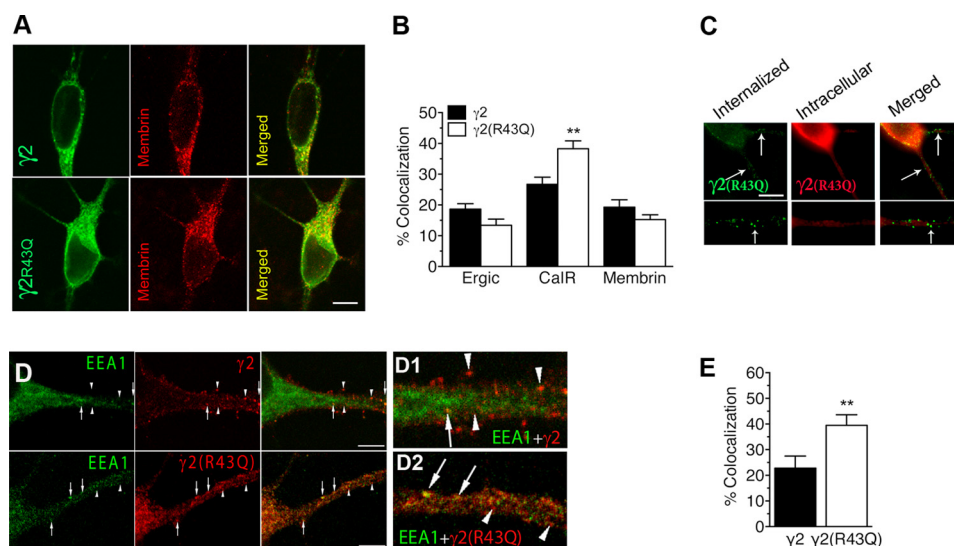


FIGURE 1. GABA_ARs containing $\gamma 2(R43Q)$ are found in internalized compartments. *A*, cultured hippocampal neurons were transfected with $\gamma 2^{Myc}$ or $\gamma 2^{Myc}(R43Q)$ subunits and stained for Myc tag together with a *cis*-Golgi compartment marker (membrin) and analyzed by confocal microscopy. *B*, quantitative analyses of the colocalization of $\gamma 2$ subunits with intracellular compartments (Ergic, endoplasmic reticulum-Golgi intermediate compartment; CalR, endoplasmic reticulum; membrin, *cis*-Golgi), normalized to Myc tag total immunoreactivity. *C*, live neurons expressing $\gamma 2^{Myc}(R43Q)$ were incubated with a monoclonal Myc antibody and FITC-conjugated secondary antibodies (left) at 37 °C, and then the fixed, permeabilized neurons were labeled with a polyclonal antibody and Alexa Fluor-568-conjugated secondary antibodies (middle). Merged images revealed intracellular punctate labeling corresponding to internalized receptors within a transfected neuron (arrows). *D*, cultured hippocampal neurons were transfected with $\gamma 2^{Myc}$ and $\gamma 2^{Myc}(R43Q)$ subunits and stained for Myc tag together with an early endosome marker (EEA1). Arrowheads, labeled subunits not colocalized with EEA1; arrows, colocalized staining. *E*, quantitative analyses of the colocalization of $\gamma 2$ subunits with EEA1, normalized to Myc tag total immunoreactivity. Scale bars, 40 μm (A and C) or 20 μm (D). **, $p < 0.005$. Error bars, S.E.

15.2 \pm 1.6% for the $\gamma 2(R43Q)$ -containing receptor, $n = 35$ and 38, respectively; ERGIC: 18.6 \pm 1.7% for the wild-type versus 13.4 \pm 1.9% for the $\gamma 2(R43Q)$ -containing receptor, $n = 28$ and 34, respectively). We therefore checked whether the absence of surface labeling was due to fast endocytosis mechanisms, as proposed to explain the exclusion of sodium channels from somatic domains (45). When living neurons, expressing $\gamma 2(R43Q)$, were incubated at 37 °C with antibodies directed against the tagged extracellular N-terminal $\gamma 2$ -domain, intracellular punctate labeling was detected (Fig. 1C), suggesting receptor internalization. This was confirmed by the increased colocalization of $\gamma 2(R43Q)$ with EEA1, an early endosome marker (Fig. 1, D and E) (22.8 \pm 4.7% for the wild-type versus 39.5 \pm 4.1% for the $\gamma 2(R43Q)$ -containing receptor, $n = 14$ and 16, respectively, $p < 0.005$).

Because clathrin-mediated, dynamin-dependent endocytosis is the major neuronal GABA_AR internalization mechanism (4, 6), we tested whether $\gamma 2(R43Q)$ internalization was driven by a similar pathway. When dynamin was inhibited by incubation with 80 μM dynasore (46), $\gamma 2(R43Q)$ was detected at the plasma membrane of transfected COS-7 cells (Fig. 2A). The ratio of $\gamma 2(R43Q)$ subunit labeled on the cell surface versus $\gamma 2(R43Q)$ labeled within intracellular compartments was increased from 0.42 \pm 0.2 to 0.78 \pm 0.18 (Fig. 2B). COS-7 cells were then transfected with a $\beta 2(LL/AA)$ mutant; this mutation within the $\beta 2$ intracellular domain reduces the interaction of GABA_AR with the AP2 complex (6). In this case, the signal ratio between surface and intracellular $\gamma 2(R43Q)$ increased from 0.18 \pm 0.08 to 0.53 \pm 0.1 (Fig. 2, C and D), showing that $\gamma 2(R43Q)$ was present on the cell surface when co-expressed with $\alpha 1$ and $\beta 2(LL/AA)$. Taken together, these data showed that the $\gamma 2$ subunit containing the R43Q mutation increased

endocytosis of GABA_ARs, hindering their detection on the cell surface.

$\gamma 2(R43Q)$ Endocytosis Is Inhibited by GABA_AR Antagonists—This increased internalization of a ligand-gated channel, resulting from a mutation within the extracellular domain of the molecular complex, was surprising. This GABA_AR domain contains binding sites for agonists and allosteric modulators, whereas the intracellular domain mediates interactions with trafficking factors (1, 4, 6, 47). We therefore tested whether GABA_AR ligands interfered with endocytosis. Incubating transfected neurons (Fig. 3, A and B) or COS-7 cells (Fig. 3, C and D) with two different antagonists (*i.e.* picrotoxin and gabazine) for 1 h significantly increased $\gamma 2(R43Q)$ surface expression, whereas neither GABA_AR agonist nor antagonists altered surface expression levels of receptors containing wild-type $\gamma 2$ subunit. The area of clusters on the surface of neurons transfected with $\gamma 2$ was 2.23 \pm 0.23 $\mu m^2/10 \mu m$ in control conditions and 2.50 \pm 0.19 or 2.36 \pm 0.16 in the presence of gabazine (100 μM) or picrotoxin (100 μM), respectively (Fig. 3B). The area of clusters on the surface of neurons transfected with $\gamma 2(R43Q)$ was 0.08 \pm 0.02 $\mu m^2/10 \mu m$ in control conditions and increased to 0.79 \pm 0.15 and 0.79 \pm 0.12 in the presence of gabazine (100 μM) or picrotoxin (100 μM), respectively (Fig. 3B). In COS-7 cells transfected with $\alpha 1$ -, $\beta 2$ -, and $\gamma 2$ subunits, the surface/intra ratio were 3.8 \pm 0.5 in control conditions and 4 \pm 0.9 or 3.3 \pm 0.4 in the presence of gabazine (100 μM) or picrotoxin (100 μM), respectively (Fig. 3D). In COS-7 cells transfected with $\alpha 1$, $\beta 2$, and $\gamma 2(R43Q)$ subunits, the surface/intra ratio increased from 0.3 \pm 0.1 to 1.27 \pm 0.2 for gabazine and 1.41 \pm 0.23 for picrotoxin (Fig. 3D). Muscimol (10 μM), a GABA_AR agonist, had no detectable effect, compared with the control experiments (Fig. 3, B and D). Cell surface biotinylation

$\gamma 2(R43Q)$ and GABA_AR Trafficking

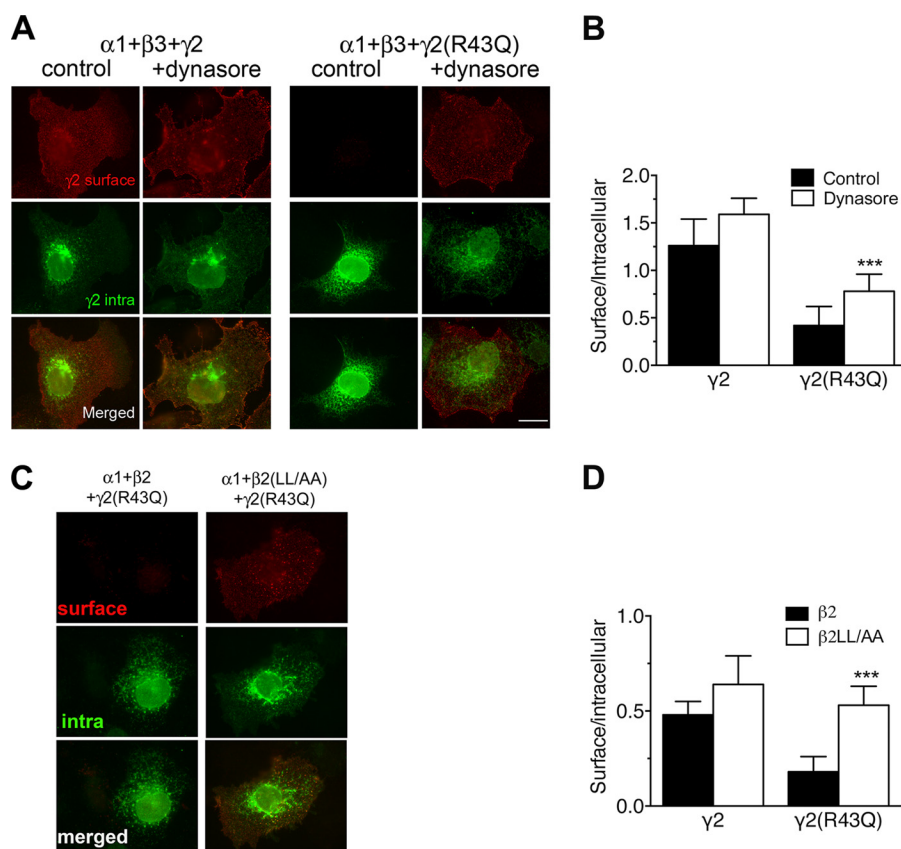


FIGURE 2. $\gamma 2(R43Q)$ internalization is clathrin- and dynamin-dependent. *A*, COS-7 cells were transiently co-transfected with $\alpha 1$ -, $\beta 3$ -, and Myc-tagged $\gamma 2$ subunits (1:1:1 ratio), either wild-type ($\gamma 2$) or bearing the R43Q ($\gamma 2(R43Q)$) substitution, as indicated at the top. Surface labeling was obtained after immunostaining living cells with a polyclonal antibody directed at the extracellular Myc tag and Alexa Fluor-568-conjugated secondary antibodies (*surface*), and intracellular staining of the same cells was revealed using a monoclonal antibody directed at the same tag and FITC-conjugated secondary antibodies (*intra*). *Merged images* show intracellular retention of the $\gamma 2(R43Q)$ subunit (*control*), whereas surface labeling was detected when cells were incubated with dynasore. *Scale bar*, 10 μm . *B*, the ratio of surface/total expression was measured in COS-7 cells expressing $\alpha 1\beta 3\gamma 2$ GABA_ARs, after incubation with dynasore ($n = 13-22$). *C*, cells were transiently co-transfected with $\alpha 1$ -, $\beta 2$ -, or $\beta 2LL/AA$ and Myc-tagged $\gamma 2$ subunit (1:1:1 ratio), either wild-type ($\gamma 2$) or bearing the R43Q ($\gamma 2(R43Q)$) substitution, as indicated at the top. Surface and intracellular labeling were obtained as above. *Merged images* show intracellular retention of the $\gamma 2(R43Q)$ subunit when cells were co-transfected with $\beta 2$, whereas surface labeling was detected when cells were co-transfected with $\beta 2LL/AA$. *Scale bar*, 10 μm . *D*, quantitative analysis of $\alpha 1\beta 2\gamma 2$ and $\alpha 1\beta 2(LL/AA)\gamma 2$ GABA_ARs surface expression in transfected COS-7 cells, ($n = 48-65$). ***, $p < 0.001$. Error bars, S.E.

on $\alpha 1$ -, $\beta 2$ -, and $\gamma 2$ -transfected COS-7 cells was not modified by 100 μM gabazine + picrotoxin treatment ($107 \pm 4\%$), whereas experiments on $\alpha 1$ -, $\beta 2$ -, and $\gamma 2(R43Q)$ -transfected cells confirmed that antagonist treatment increased significantly the surface fraction of $\gamma 2(R43Q)$ ($213 \pm 29\%$ of control, $p < 0.05$, three independent experiments; Fig. 3, *E* and *F*).

The fact that picrotoxin and gabazine are both allosteric GABA_AR antagonists (48–50) indicated that, compared with their wild-type counterparts, the equilibrium between states in $\gamma 2(R43Q)$ -containing GABA_ARs shifted away from the resting state toward the active or desensitized state. Our new homology model based on a glutamate-gated chloride channel (42) suggests that the Arg-43 residue of the $\gamma 2$ subunit is connected to Tyr = 174 and Glu-178 from the loop B and to Asp-84 and Arg-86 of the $\beta 2$ subunit via polar interactions (Fig. 4, *B–D*). In addition, this new model shows that $\gamma 2$ Arg-43 and $\beta 2$ Asp-84/Arg-86 are on loops (Allo1 and Allo2) identified as involved in the motion that opens the channel pore (51). This prompted us to test whether this alteration in the equilibrium between states favored an open channel conformation. We thus co-expressed wild-type or $\gamma 2(R43Q)$ constructs with $\alpha 1$ and $\beta 2$ subunits in HEK cells. In $\alpha 1$ -, $\beta 2$ -, and $\gamma 2(R43Q)$ -transfected cells, maxi-

mum GABA-gated currents were 16% ($p < 0.01$) of currents from cells expressing wild-type receptors (Fig. 4*E*), in agreement with previous findings (19, 23, 52). Gabazine, an allosteric antagonist, did not cause a significant change in the current base line during whole cell voltage clamp recordings (Fig. 4*F*) in HEK cells co-expressing $\alpha 1$ -, $\beta 2$ -, and either wild-type or $\gamma 2(R43Q)$ subunits ($n = 7$ and 15, respectively), showing that $\gamma 2(R43Q)$ -containing receptors had no constitutive activity.

Collectively, our data suggested that $\gamma 2(R43Q)$ mutation triggered GABA_AR endocytosis through a structural change in the extracellular domain. Because agonist exposure triggers a long range conformational change (53, 54), our finding on mutated receptors opened the interesting possibility that endocytosis of wild-type GABA_ARs may be modulated by agonists. Our data did not yet indicate significant alteration of the surface level of wild-type $\gamma 2$ -containing receptors in the presence of agonists (Fig. 3). We thus decided to examine directly the impact of agonists on the internalized fraction of GABA_ARs.

GABA_AR Agonist Enhances Receptor Endocytosis—To test a possible link between GABA-induced conformational change and endocytosis, suggested by our studies on $\gamma 2(R43Q)$, we directly quantified internalization by measuring the level of

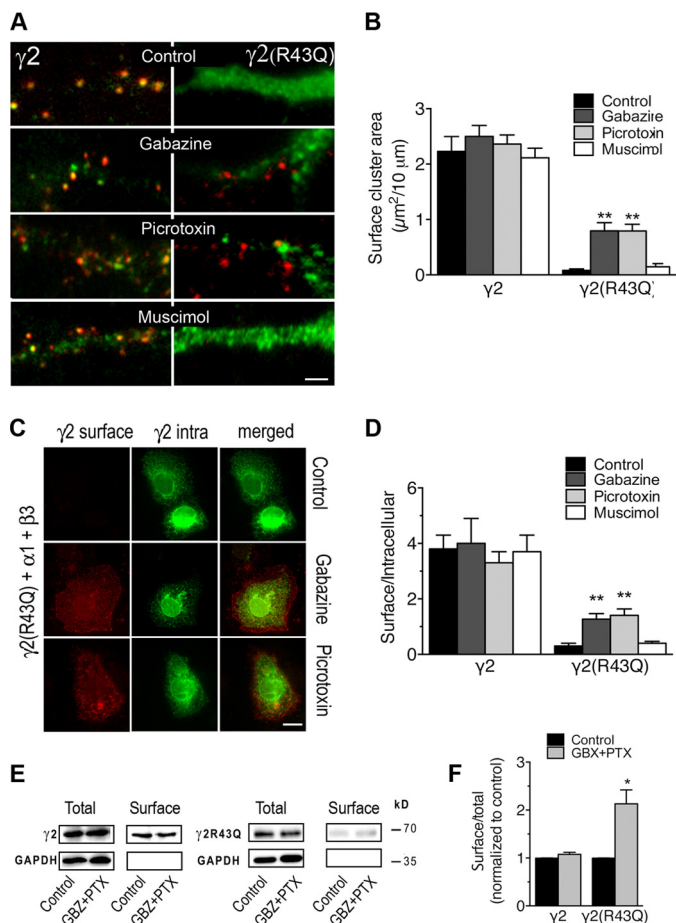


FIGURE 3. $\gamma 2(R43Q)$ internalization is inhibited by GABA_AR antagonists. *A* and *B*, neurons were transfected with $\gamma 2^{Myc}$ or $\gamma 2^{Myc}(R43Q)$ subunits. Surface labeling was obtained after immunostaining live neurons at 20 °C with a polyclonal antibody directed at the extracellular Myc tag and Alexa Fluor-568-conjugated secondary antibodies. Intracellular staining of the same cells was obtained after permeabilization and labeling with a monoclonal antibody directed at the same tag and FITC-conjugated secondary antibodies. *A*, merged images revealed the $\gamma 2(R43Q)$ subunit on the surface of transfected neurons when cells were incubated with gabazine or picrotoxin at 37 °C for 1 h prior to immunostaining. Scale bar, 10 μm. *B*, quantitative analyses of the surface cluster area formed by $\gamma 2$ constructs ($n = 13-32$). **, $p < 0.005$. *C* and *D*, COS-7 cells were transiently co-transfected with $\alpha 1$ -, $\beta 3$ -, and Myc-tagged $\gamma 2$ subunits, either wild-type ($\gamma 2$) or bearing the R43Q ($\gamma 2(R43Q)$) substitution. Treatment and labeling were as in *A*, and the surface/total expression ratio (*D*) was calculated as the ratio of the surface Alexa Fluor-568 fluorescence level on live cells to FITC fluorescence on permeabilized cells ($n = 12-25$). **, $p < 0.005$. *E* and *F*, COS-7 cells were transfected with $\alpha 1$ -, $\beta 2$ -, and Myc-tagged $\gamma 2$ or $\gamma 2(R43Q)$ subunits and incubated with or without picrotoxin and gabazine 30 min before surface biotinylation. *E*, representative Western blot shows Myc-tagged $\gamma 2$ and $\gamma 2(R43Q)$ immunoreactivity in total or surface-biotinylated extracts from transfected cells. *F*, means of surface/total expression ratio from three independent experiments normalized to values of total $\gamma 2$ or $\gamma 2(R43Q)$, as indicated, described in *E* show that treatment by picrotoxin and gabazine increases the surface-biotinylated fraction of cells expressing the $\gamma 2$ subunit bearing the R43Q mutation. *, $p < 0.01$. Error bars, S.E.

endogenous $\alpha 1$ -containing receptors internalized during agonist application on cultured neurons (Fig. 5A). In control and muscimol experiments, excitatory activity was blocked with 6-cyano-7-nitroquinoxaline-2,3-dione, D-2-amino-5-phosphonovaleric acid, and tetrodotoxin in the medium. Neurons were incubated with an antibody directed at the extracellular N-terminal domain of $\alpha 1$ subunit for 30 min at 37 °C. Labeled receptors remaining at the cell surface were labeled with saturating concentration of Alexa Fluor-647 secondary antibodies,

internalized receptors were labeled with Alexa Fluor-488 secondary antibodies (Fig. 5A, green), whereas total $\alpha 1$ subunits were labeled with a monoclonal antibody and Alexa Fluor-568 secondary antibodies (Fig. 5A, red). Quantification of the area of punctate labeling of internalized receptors showed a significant increase when neurons were incubated with 10 μM muscimol (the area of intracellular punctate labeling/10 μm increased to $3.14 \pm 0.36 \mu m^2$ from 1.62 ± 0.17 in control condition). This increase was abolished when muscimol was co-applied with 100 μM gabazine or picrotoxin (1.68 ± 0.15 or $1.89 \pm 0.18 \mu m^2$, respectively). Application of gabazine or picrotoxin alone had no effect (1.69 ± 0.19 or $1.61 \pm 0.16 \mu m^2$, respectively) (Fig. 5B).

In another set of experiments, we analyzed $\gamma 2$ subunit internalization in COS cells transfected with $\alpha 1$, $\beta 2$, and tagged $\gamma 2$ subunits (Fig. 6A). Average values \pm S.E. from four independent experiments and 105 cells for each condition were plotted (Fig. 6B). These experiments showed that the number of internalized $\gamma 2$ subunits increased during agonist treatment. The area of intracellular punctate labeling rose from $21.41 \pm 3.28 \mu m^2$ in the control cells to $59.70 \pm 6.89 \mu m^2$ when cells were treated with 100 μM GABA at 37 °C for 30 min. This increase was abolished when GABA was applied with gabazine, picrotoxin, or picrotoxin + gabazine (27.36 ± 3.29 , 21.72 ± 2.82 , or $21.41 \pm 3.28 \mu m^2$, respectively). When compared with control, gabazine or picrotoxin had no significant effect on the area of intracellular punctate labeling (36.39 ± 5.42 or 28.89 ± 4.09 , respectively).

We also assessed $\gamma 2$ internalization by performing a biotinylation assay on COS-7 cells transfected as above. After labeling with cleavable biotin, plates were returned to 37 °C for 30 min to allow endocytosis. Cells were then exposed to MESNA, which cleaved biotin from proteins remaining on the surface, allowing determination of intracellular biotinylated receptors. As shown in Fig. 6, C and D, application of GABA induced a significant increase of the internalization ($212 \pm 40\%$ of control, $n = 6$, $p < 0.05$) that was suppressed when antagonists were co-applied with GABA ($99.5 \pm 27\%$).

We next examined whether agonist-induced internalization reduced the amount of receptors on the cell surface (Fig. 6E) by surface biotinylation experiments. Comparison of the relative surface/total ratio, in the absence or the presence of GABA (Fig. 6, E and F), showed that the ligand did not change significantly the amount of receptors on the surface. Expression is normalized to 1 for control and is 1.08 ± 0.11 for GABA-treated cells and 1.06 ± 0.12 for antagonist-treated cells; $n = 3$ independent experiments (Fig. 6F). These data implied that GABA_AR endocytosis may be compensated for by exocytosis or reinsertion of GABA_ARs. Indeed, inhibition of receptor recycling with monensin (55, 56) (Fig. 6G) reduced significantly the surface expression of GABA_ARs following application of 10 μM muscimol. Expression is normalized to 1 for control and is 0.722 ± 0.034 for muscimol-treated cells (80 cells for each condition, five independent experiments), suggesting that removal and insertion of GABA_ARs on the cell surface is a use-dependent process that is tightly regulated.

$\gamma 2(R43Q)$ and $GABA_A R$ Trafficking

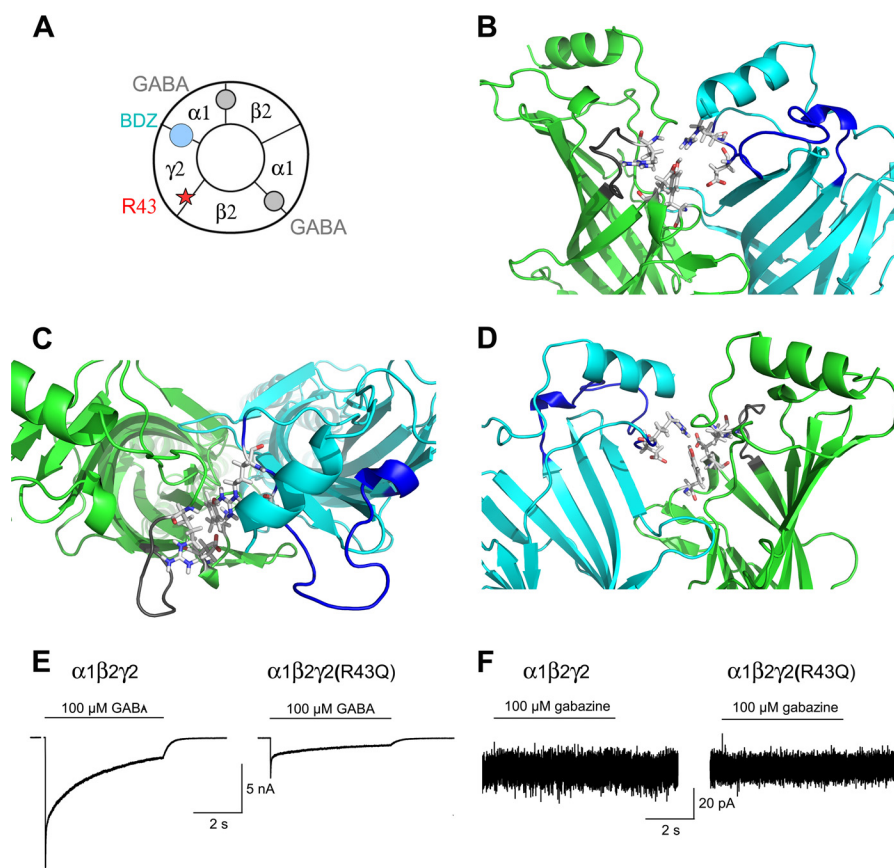


FIGURE 4. The $\gamma 2(R43Q)$ mutation is not associated with an open channel conformation. *A*, schematic diagram of an $\alpha 1 \beta 2 \gamma 2$ $GABA_A R$, which illustrates the five combined subunits that form the complex, the two GABA active binding sites at the $\beta 2$ and $\alpha 1$ interfaces (gray circles), and the benzodiazepine (BDZ; blue circle) allosteric binding site at the $\alpha 1$ and $\gamma 2$ interface. In current models, $\gamma 2$ Arg-43 is at the interface with $\beta 2$. *B–D*, $GABA_A R$ model viewed from the outside (*B*), the top (*C*), and inside (*D*); only the $\gamma 2$ and $\beta 2$ subunits are shown for clarity ($\gamma 2$ in green and $\beta 2$ in blue). $\gamma 2$ (Arg-43, Tyr-174, and Glu-178) and $\beta 2$ (Asp-84 and Arg-86) residues are represented by sticks. These residues are within loops, shown in gray ($\gamma 2$ subunit) or dark blue ($\beta 2$), identified as being involved in the channel-opening motion. *E*, GABA application on HEK cells transfected with $\alpha 1 \beta 2 \gamma 2$ or $\alpha 1 \beta 2 \gamma 2(R43Q)$ activated membrane currents, whereas gabazine application (*F*) did not change the holding current in either type of receptor.

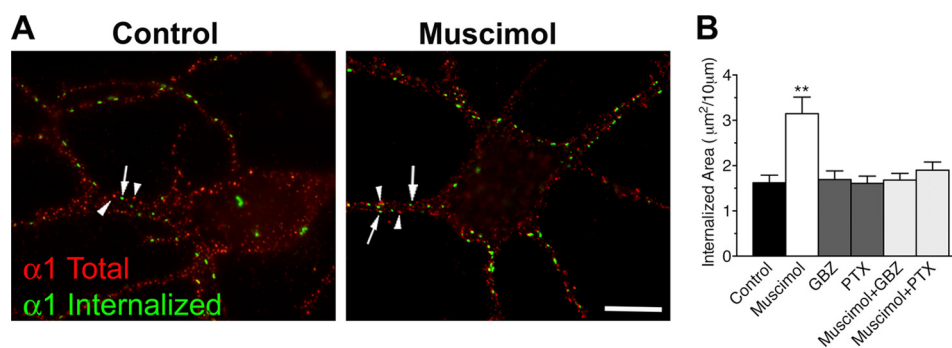


FIGURE 5. $GABA_A R$ internalization in neurons is increased by muscimol. *A*, internalized labeling was obtained after incubating live cultured hippocampal neurons with a polyclonal antibody directed at the extracellular domain of the native $\alpha 1$ subunit at $37^\circ C$ (Internalized). Total staining of the same neurons was performed after permeabilization and labeling with a monoclonal antibody directed at the intracellular domain of the native $\alpha 1$ subunit (total). Arrows, labeling of internalized receptors; arrowheads, labeling of the intracellular domain. Scale bar, $10 \mu m$. *B*, quantitative analysis of the area of intracellular punctate labeling of internalized receptors formed by $\alpha 1$ subunits in dendrites of neurons incubated in culture medium (control), with muscimol, gabazine (gbz), or picrotoxin (ptx); a total of four experiments on independent neuron cultures where carried out, with the number of quantified neurons going from $n = 32$ to 40 . **, $p < 0.005$. Error bars, S.E.

DISCUSSION

Modulation of surface stability of $GABA_A R$ s is essential for regulating the physiological properties of inhibitory neurotransmission. Modification of inhibitory signaling and altered receptor trafficking has been associated with several neurological diseases, including schizophrenia, substance abuse, pain, or epilepsy (2, 11, 57–61). It is also established that

$GABA_A R$ s endocytosis is regulated through intracellular signaling pathways (1, 2, 4). Here we show that a mutation in the N-terminal domain and ligand application have both an influence on receptor endocytosis. Thus, our data uncover a mechanism that links the extracellular domain of $GABA_A R$ s to their stability on the cell surface. It must be noted that it was possible that we had detected the traffic of recombinant $\gamma 2$ subunits in

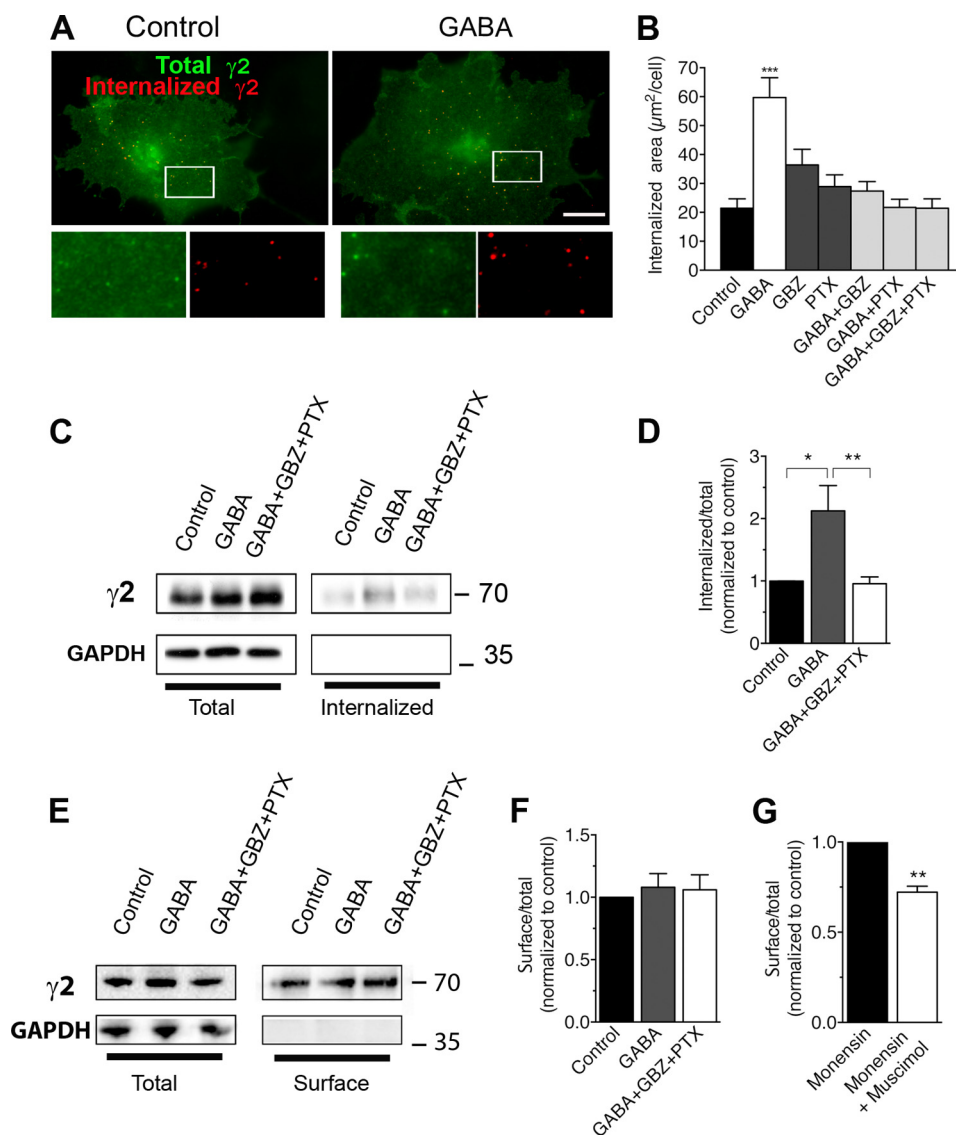


FIGURE 6. GABA_AR internalization in COS-7 cells is increased by GABA. A, COS-7 cells were transiently co-transfected with $\alpha 1$ -, $\beta 2$ -, and Myc-tagged $\gamma 2$ subunits. Internalized labeling (red) was obtained after incubating live cells with polyclonal antibody directed at the extracellular Myc tag at 37 °C followed by stripping of antibodies remaining on the surface. Intracellular staining (green) of the same cells was obtained after permeabilization and labeling with a monoclonal antibody directed at the same tag (white frames detailed in lower panels). Scale bar, 10 μ m. B, quantification of the area of intracellular punctate labeling of internalized receptors formed by $\gamma 2$ subunit in cells incubated in culture medium (Ctrl) with GABA, gabazine (GBZ), or picrotoxin (PTX). ***, $p < 0.001$. C, COS-7 cells transfected as in A were labeled with biotin and returned to 37 °C in control medium, GABA, gabazine, or picrotoxin, as indicated. Biotin remaining on the surface after the incubation at 37 °C was removed by cleaving. Total and internalized (biotinylated) $\gamma 2$ subunits were detected with an anti-Myc antibody. GAPDH staining shows that intracellular proteins were not biotinylated. D, means of internalized/total expression ratio normalized to total $\gamma 2$ from experiments described in C. **, $p < 0.005$; *, $p < 0.01$. E, COS-7 cells transfected as in A and C and labeled with biotin. Representative Western blot shows Myc-tagged $\gamma 2$ in total or surface-biotinylated extracts. F, means of surface/total expression ratio normalized to total $\gamma 2$ from experiments described in E show that surface expression was unchanged by treatment with GABA. G, quantitative analysis of $\alpha 1\beta 2\gamma 2$ GABA_AR surface expression in COS-7 cells transiently co-transfected with $\alpha 1$ -, $\beta 2$ -, and Myc-tagged $\gamma 2$ subunits and incubated with monensin with or without muscimol for 30 min before surface and total immunofluorescence labeling. A value of 1 for cells incubated without muscimol was used. **, $p < 0.005$. Error bars, S.E.

monomer form because it has been shown in some heterologous cells transfected with this subunit alone. However, we have previously shown that this is unlikely (22). Furthermore, in the present work, we found that the amount of $\gamma 2(R43Q)$ detected on the cell surface increased in the presence of a $\beta 2$ subunit bearing the LL/AA substitution or following treatment with gabazine, a competitive antagonist of the GABA binding site. Because $\beta 2(LL/AA)$ should be associated with $\gamma 2(R43Q)$ to increase cell surface labeling and the gabazine binding site is within the interface between α and β subunits (48), these exper-

iments strongly suggest that $\gamma 2(R43Q)$ detected on the cell surface is part of an oligomer also containing α and β subunits. The same holds true for wild type $\gamma 2$ subunit endocytosis promoted by GABA (or muscimol), the binding site of which is at the α/β interface (Fig. 4A).

Analysis of $\gamma 2(R43Q)$ fate in neurons showed an increased retention in the endoplasmic reticulum, in agreement with previous findings in human embryonic kidney 293-T cells (24). Additionally, we provide evidence that $\gamma 2(R43Q)$ is not entirely retained within the reticulum and is transported via

$\gamma 2(R43Q)$ and GABA_AR Trafficking

the Golgi apparatus to the cell membrane, where mutated receptors are highly internalized via a clathrin- and dynamin-dependent mechanism. Blockade of endocytosis leads to a major increase in $\gamma 2(R43Q)$ surface targeting in neurons and COS-7 cells, indicating that internalization is a major mechanism for down-regulating cell surface expression of $\gamma 2(R43Q)$ -containing receptors.

We also show that gabazine or picrotoxin increases dramatically the surface expression of $\gamma 2(R42Q)$ subunit. These two GABA_AR antagonists are both negative allosteric modulators, acting at different sites (48–50, 62). The gabazine- and picrotoxin-sensitive internalization of $\gamma 2(R43Q)$ suggested that endocytosis could be linked to a constitutive activity of the mutated receptor. Electrophysiological recordings of $\gamma 2(R43Q)$ -expressing cells clearly showed that this mutated subunit did not give rise to constitutive currents. Therefore, the effect of antagonists on $\gamma 2(R43Q)$ endocytosis is probably related to another conformational state (e.g. the desensitized state). Interestingly, it has been shown that the $\gamma 2(R43Q)$ mutation favors desensitized states (52).

Consequently, our findings, showing that GABA_AR antagonists prevent $\gamma 2(R43Q)$ endocytosis, suggest that internalization is driven by a global conformational change. Molecular models show that the $\gamma 2$ Arg-43 residue is at the $\gamma 2/\beta 2$ interface in the extracellular domain, on a loop positioned above the pocket, which is homologous to the GABA binding sites. Interestingly, many mutations in nicotinic receptors linked to diseases are at the interface between receptor subunits (63); they alter the gating allosterically (i.e. from a distance) (63–64). A model indicates that $\gamma 2$ Arg-43 and $\gamma 2$ Glu-178 are connected through a bifurcated salt bridge; this model has been used to study the $\gamma 2(R43Q)$ mutation (22, 26, 52). One of these studies has suggested that these positions have a long range allosteric effect (52). In our new GABA_AR model derived from the glutamate-gated chloride channel (42), the Arg-43 residue of the $\gamma 2$ subunit is connected to Tyr-174 and Glu-178 from the loop B and to the $\beta 2$ subunit via polar interactions that should be sensitive to the R43Q substitution and positioned on a loop thought to be involved in the channel pore opening motion (51). Moreover, electrophysiological recordings and kinetic analyses have shown that the long distance effects of $\gamma 2(R43Q)$ substitution extend as far as the transmembrane domains (52). Therefore, $\gamma 2(R43Q)$ mutation might have an influence on receptor endocytosis in line with the current views on pentameric ligand-gated ion channels, describing a link between extracellular, transmembrane, and intracellular domains (53, 65, 66).

Because ligand binding in the Cys-loop receptor family is followed by a whole chain of interconnections, including the intracellular domain (67), it is of interest to assess whether GABA binding may influence GABA_AR endocytosis. Although it is established that the number of surface GABA_ARs is regulated by constitutive endocytosis and neuromodulation through intracellular signaling (5–8, 68, 69), previous findings on ligand-independent or -dependent internalization are conflicting (28–31). Several studies have investigated GABA_A receptor internalization following agonist application (29, 30). However, data were obtained by analyzing the amount of receptors

remaining at the surface after agonist application. Here, we used a different approach (i.e. quantification of internalized receptors). Altogether, biochemical and immunocytochemical analyses of internalized receptor fraction, both in neurons and in COS-7, showed an increased number of internalized receptors during agonist application (Figs. 5B and 6, B and D), whereas the surface/intracellular ratio or surface labeling (Figs. 3, B and D, and 6E) remained unchanged. These data show that an overall counting of receptors on the cell membrane may overlook an increased endocytosis.

It has been suggested that internalization of GABA_ARs or increase in neuronal activity is accompanied by insertion of new receptors (4, 7, 70–72). Here, all of the experiments performed on neurons were conducted in the presence of tetrodotoxin and glutamate receptor inhibitors, suggesting that agonist binding endocytosis associated with the insertion of new receptors should instead represent an additional homeostasis mechanism. Knowing that internalized receptors are recycled back to the surface membrane or targeted for degradation and that endocytosis may be compensated for by surface targeting of distinct receptor subtypes, this balance between agonist-induced removal and insertion of receptors may regulate the number, but also the identity, of GABA_ARs on the cell surface. Because the functional and pharmacological properties of GABA_ARs depend on subunit composition, our findings showing that ligand stimulation increased endocytosis imply that this mechanism may be an important process for a fine tuning of GABAergic neurotransmission (4). It is of note that benzodiazepines (allosteric modulators of GABA_ARs) induce a subtype-specific change via enhanced degradation rather than alterations in receptor insertion or endocytosis, thus revealing another mechanism that might regulate GABAergic neurotransmission (73).

The $\gamma 2(R43Q)$ mutation is directly linked to epilepsy (16, 17). Thus, our findings, revealing a direct relationship between receptor endocytosis and a neurological disorder, are in line with the emerging concept that GABA_AR trafficking deficiencies are key factors in initiating and maintaining several diseases, including epilepsy (4, 6, 15). For example, status epilepticus leads to enhanced GABA_AR endocytosis (28–30). The K289M substitution in the $\gamma 2$ subunit known to be responsible for generalized epilepsy with febrile seizures plus alters the membrane diffusion of GABA_ARs (61). It must be also noted that a shortened lifetime caused by the epilepsy mutation A322D on $\alpha 1$ -containing GABA_ARs has been proposed (74) (but also see Ref. 75). Interestingly, experiments on $\gamma 2(R43Q)$ knock-in mice and transfected neurons or COS-7 cells have shown that $\alpha 1$ and $\alpha 3$ subunit surface expression was not reduced, despite a dramatic decrease in $\gamma 2(R43Q)$ surface labeling (16, 22). Earlier data, together with our present findings, show that the consequence of the mutation is a complex and dynamic process, suggesting that the defect is an active phenomenon instead of a more static retention of mutated receptors in the intracellular compartments and that $\gamma 2(R43Q)$ -containing receptor internalization is associated with a compensatory insertion of distinct GABA_AR subtypes.

CONCLUSION

$\gamma 2(R43Q)$ -containing GABA_ARs are in a conformational state that promotes internalization, providing evidence for a direct link between GABA_AR endocytosis and epilepsy. Furthermore, our data suggest that GABA_AR endocytosis is use-dependent, consistent with a model in which ligand binding induces a conformation of the receptor that is a substrate for the biochemical events leading to endocytosis (70). Because GABA is the main inhibitory neurotransmitter in the brain and GABA_ARs are the target of many drugs, this property may have important functional and pathophysiological implications and should therefore be fully characterized (1, 4). Our data suggest that the $\gamma 2(R43Q)$ mutant is a useful model for this purpose. Our findings also illustrate the fact that mutations offer insights not only into diseases but also receptor physiology (61, 64, 74, 76). It would be also of interest to assess whether the different allosteric drugs acting on GABA_ARs have an influence on receptor trafficking.

Acknowledgments—We thank Dr. Daniel Choquet for helpful discussions, Christel Poujol for expertise with imaging, Erwin Sigel for human $\alpha 1$ cDNA, and Laura Cardoit and Frederique Masmjean for technical assistance.

REFERENCES

- Luscher, B., Fuchs, T., and Kilpatrick, C. L. (2011) GABA_A receptor trafficking-mediated plasticity of inhibitory synapses. *Neuron* **70**, 385–409
- Smith, K. R., and Kittler, J. T. (2010) The cell biology of synaptic inhibition in health and disease. *Curr. Opin. Neurobiol.* **20**, 550–556
- Triller, A., and Choquet, D. (2008) New concepts in synaptic biology derived from single-molecule imaging. *Neuron* **59**, 359–374
- Jacob, T. C., Moss, S. J., and Jurd, R. (2008) GABA_A receptor trafficking and its role in the dynamic modulation of neuronal inhibition. *Nat. Rev. Neurosci.* **9**, 331–343
- Kittler, J. T., Delmas, P., Jovanovic, J. N., Brown, D. A., Smart, T. G., and Moss, S. J. (2000) Constitutive endocytosis of GABA_A receptors by an association with the adaptin AP2 complex modulates inhibitory synaptic currents in hippocampal neurons. *J. Neurosci.* **20**, 7972–7977
- Leidenheimer, N. J. (2008) Regulation of excitation by GABA_A receptor internalization. *Results Probl. Cell Differ.* **44**, 1–28
- Bannai, H., Lévi, S., Schweizer, C., Inoue, T., Launey, T., Racine, V., Sibarita, J. B., Mikoshiba, K., and Triller, A. (2009) Activity-dependent tuning of inhibitory neurotransmission based on GABA_AR diffusion dynamics. *Neuron* **62**, 670–682
- Kittler, J. T., Thomas, P., Tretter, V., Bogdanov, Y. D., Haucke, V., Smart, T. G., and Moss, S. J. (2004) Huntingtin-associated protein 1 regulates inhibitory synaptic transmission by modulating γ -aminobutyric acid type A receptor membrane trafficking. *Proc. Natl. Acad. Sci. U.S.A.* **101**, 12736–12741
- Smith, K. R., Muir, J., Rao, Y., Browarski, M., Gruenig, M. C., Sheehan, D. F., Haucke, V., and Kittler, J. T. (2012) Stabilization of GABA_A receptors at endocytic zones is mediated by an AP2 binding motif within the GABA_A receptor $\beta 3$ subunit. *J. Neurosci.* **32**, 2485–2498
- Cossart, R., Bernard, C., and Ben-Ari, Y. (2005) Multiple facets of GABAergic neurons and synapses. Multiple fates of GABA signalling in epilepsies. *Trends Neurosci.* **28**, 108–115
- Fritschy, J. M. (2008) Epilepsy, E/I balance and GABA_A receptor plasticity. *Front. Mol. Neurosci.* **1**, 5
- Li, H., Kraus, A., Wu, J., Huguenard, J. R., and Fisher, R. S. (2006) Selective changes in thalamic and cortical GABA_A receptor subunits in a model of acquired absence epilepsy in the rat. *Neuropharmacology* **51**, 121–128
- Meldrum, B. S., and Rogawski, M. A. (2007) Molecular targets for antiepileptic drug development. *Neurotherapeutics* **4**, 18–61
- Noebels, J. L. (2003) The biology of epilepsy genes. *Annu. Rev. Neurosci.* **26**, 599–625
- Ragozzino, D., Palma, E., Di Angelantonio, S., Amici, M., Mascia, A., Arcella, A., Giangaspero, F., Cantore, G., Di Gennaro, G., Manfredi, M., Esposito, V., Quarato, P. P., Miledi, R., and Eusebi, F. (2005) Rundown of GABA type A receptors is a dysfunction associated with human drug-resistant mesial temporal lobe epilepsy. *Proc. Natl. Acad. Sci. U.S.A.* **102**, 15219–15223
- Tan, H. O., Reid, C. A., Single, F. N., Davies, P. J., Chiu, C., Murphy, S., Clarke, A. L., Dibbens, L., Krestel, H., Mulley, J. C., Jones, M. V., Seeburg, P. H., Sakmann, B., Berkovic, S. F., Sprengel, R., and Petrou, S. (2007) Reduced cortical inhibition in a mouse model of familial childhood absence epilepsy. *Proc. Natl. Acad. Sci. U.S.A.* **104**, 17536–17541
- Wallace, R. H., Marini, C., Petrou, S., Harkin, L. A., Bowser, D. N., Panchal, R. G., Williams, D. A., Sutherland, G. R., Mulley, J. C., Scheffer, I. E., and Berkovic, S. F. (2001) Mutant GABA_A receptor $\gamma 2$ -subunit in childhood absence epilepsy and febrile seizures. *Nat. Genet.* **28**, 49–52
- Bailey, M. E., Matthews, D. A., Riley, B. P., Albrecht, B. E., Kostrzewa, M., Hicks, A. A., Harris, R., Müller, U., Darlison, M. G., and Johnson, K. J. (1999) Genomic mapping and evolution of human GABA_A receptor subunit gene clusters. *Mamm. Genome* **10**, 839–843
- Bianchi, M. T., Song, L., Zhang, H., and Macdonald, R. L. (2002) Two different mechanisms of disinhibition produced by GABA_A receptor mutations linked to epilepsy in humans. *J. Neurosci.* **22**, 5321–5327
- Bowser, D. N., Wagner, D. A., Czajkowski, C., Cromer, B. A., Parker, M. W., Wallace, R. H., Harkin, L. A., Mulley, J. C., Marini, C., Berkovic, S. F., Williams, D. A., Jones, M. V., and Petrou, S. (2002) Altered kinetics and benzodiazepine sensitivity of a GABA_A receptor subunit mutation ($\gamma 2(R43Q)$) found in human epilepsy. *Proc. Natl. Acad. Sci. U.S.A.* **99**, 15170–15175
- Eugène, E., Depienne, C., Baulac, S., Baulac, M., Fritschy, J. M., Le Guern, E., Miles, R., and Poncer, J. C. (2007) GABA_A receptor $\gamma 2$ subunit mutations linked to human epileptic syndromes differentially affect phasic and tonic inhibition. *J. Neurosci.* **27**, 14108–14116
- Frugier, G., Coussen, F., Giraud, M. F., Odessa, M. F., Emerit, M. B., Boué-Grabot, E., and Garret, M. (2007) A $\gamma 2(R43Q)$ mutation, linked to epilepsy in humans, alters GABA_A receptor assembly and modifies subunit composition on the cell surface. *J. Biol. Chem.* **282**, 3819–3828
- Hales, T. G., Tang, H., Bolla, K. A., Johnson, S. J., King, D. P., McDonald, N. A., Cheng, A., and Connolly, C. N. (2005) The epilepsy mutation, $\gamma 2(R43Q)$ disrupts a highly conserved intersubunit contact site, perturbing the biogenesis of GABA_A receptors. *Mol. Cell Neurosci.* **29**, 120–127
- Kang, J., and Macdonald, R. L. (2004) The GABA_A receptor $\gamma 2$ subunit R43Q mutation linked to childhood absence epilepsy and febrile seizures causes retention of $\alpha 1\beta 2\gamma 2S$ receptors in the endoplasmic reticulum. *J. Neurosci.* **24**, 8672–8677
- Kang, J. Q., Shen, W., and Macdonald, R. L. (2006) Why does fever trigger febrile seizures? GABA_A receptor $\gamma 2$ subunit mutations associated with idiopathic generalized epilepsies have temperature-dependent trafficking deficiencies. *J. Neurosci.* **26**, 2590–2597
- Sancar, F., and Czajkowski, C. (2004) A GABA_A receptor mutation linked to human epilepsy ($\gamma 2R43Q$) impairs cell surface expression of $\alpha\beta\gamma$ receptors. *J. Biol. Chem.* **279**, 47034–47039
- Galanopoulou, A. S. (2010) Mutations affecting GABAergic signaling in seizures and epilepsy. *Pflugers Arch.* **460**, 505–523
- Barnes, E. M., Jr. (1996) Use-dependent regulation of GABA_A receptors. *Int. Rev. Neurobiol.* **39**, 53–76
- Goodkin, H. P., Joshi, S., Mtchedlishvili, Z., Brar, J., and Kapur, J. (2008) Subunit-specific trafficking of GABA_A receptors during status epilepticus. *J. Neurosci.* **28**, 2527–2538
- Naylor, D. E., Liu, H., and Wasterlain, C. G. (2005) Trafficking of GABA_A receptors, loss of inhibition, and a mechanism for pharmacoresistance in status epilepticus. *J. Neurosci.* **25**, 7724–7733
- Saito, M., Toyoda, H., Sato, H., Ishii, H., and Kang, Y. (2009) Rapid use-dependent down-regulation of γ -aminobutyric acid type A recep-

- tors in rat mesencephalic trigeminal neurons. *J. Neurosci. Res.* **87**, 3120–3133
32. Boué-Grabot, E., Emerit, M. B., Toulmé, E., Séguéla, P., and Garret, M. (2004) Cross-talk and co-trafficking between rho1/GABA receptors and ATP-gated channels. *J. Biol. Chem.* **279**, 6967–6975
33. Boué-Grabot, E., Toulmé, E., Emerit, M. B., and Garret, M. (2004) Subunit-specific coupling between γ -aminobutyric acid type A and P2X2 receptor channels. *J. Biol. Chem.* **279**, 52517–52525
34. Connolly, C. N., Krishek, B. J., McDonald, B. J., Smart, T. G., and Moss, S. J. (1996) Assembly and cell surface expression of heteromeric and homomeric γ -aminobutyric acid type A receptors. *J. Biol. Chem.* **271**, 89–96
35. Coussen, F., Normand, E., Marchal, C., Costet, P., Choquet, D., Lambert, M., Mège, R. M., and Mulle, C. (2002) Recruitment of the kainate receptor subunit glutamate receptor 6 by cadherin/catenin complexes. *J. Neurosci.* **22**, 6426–6436
36. Toulmé, E., Soto, F., Garret, M., and Boué-Grabot, E. (2006) Functional properties of internalization-deficient P2X4 receptors reveal a novel mechanism of ligand-gated channel facilitation by ivermectin. *Mol. Pharmacol.* **69**, 576–587
37. Ben-Tekaya, H., Miura, K., Pepperkok, R., and Hauri, H. P. (2005) Live imaging of bidirectional traffic from the ERGIC. *J. Cell Sci.* **118**, 357–367
38. Huyghe, D., Veran, J., Labrousse, V. F., Perrais, D., Mulle, C., and Coussen, F. (2011) Endocytosis of the glutamate receptor subunit GluK3 controls polarized trafficking. *J. Neurosci.* **31**, 11645–11654
39. Mondin, M., Carta, M., Normand, E., Mulle, C., and Coussen, F. (2010) Profilin II regulates the exocytosis of kainate glutamate receptors. *J. Biol. Chem.* **285**, 40060–40071
40. Pettrini, E. M., Lu, J., Cognet, L., Lounis, B., Ehlers, M. D., and Choquet, D. (2009) Endocytic trafficking and recycling maintain a pool of mobile surface AMPA receptors required for synaptic potentiation. *Neuron* **63**, 92–105
41. Le Novère, N., and Changeux, J. P. (1999) The Ligand Gated Ion Channel Database. *Nucleic Acids Res.* **27**, 340–342
42. Hibbs, R. E., and Gouaux, E. (2011) Principles of activation and permeation in an anion-selective Cys-loop receptor. *Nature* **474**, 54–60
43. Notredame, C., Higgins, D. G., and Heringa, J. (2000) T-Coffee. A novel method for fast and accurate multiple sequence alignment. *J. Mol. Biol.* **302**, 205–217
44. Sali, A., and Blundell, T. L. (1993) Comparative protein modelling by satisfaction of spatial restraints. *J. Mol. Biol.* **234**, 779–815
45. Fache, M. P., Moussif, A., Fernandes, F., Giraud, P., Garrido, J. J., and Dargent, B. (2004) Endocytotic elimination and domain-selective tethering constitute a potential mechanism of protein segregation at the axonal initial segment. *J. Cell Biol.* **166**, 571–578
46. Macia, E., Ehrlich, M., Massol, R., Boucrot, E., Brunner, C., and Kirchhausen, T. (2006) Dynasore, a cell-permeable inhibitor of dynamin. *Dev. Cell* **10**, 839–850
47. Wang, H., Bedford, F. K., Brandon, N. J., Moss, S. J., and Olsen, R. W. (1999) GABA_A-receptor-associated protein links GABA_A receptors and the cytoskeleton. *Nature* **397**, 69–72
48. Boileau, A. J., Newell, J. G., and Czajkowski, C. (2002) GABA_A receptor $\beta 2$ Tyr⁹⁷ and Leu⁹⁹ line the GABA-binding site. Insights into mechanisms of agonist and antagonist actions. *J. Biol. Chem.* **277**, 2931–2937
49. Ueno, S., Bracamontes, J., Zorumski, C., Weiss, D. S., and Steinbach, J. H. (1997) Bicuculline and gabazine are allosteric inhibitors of channel opening of the GABA_A receptor. *J. Neurosci.* **17**, 625–634
50. Torres, V. I., and Weiss, D. S. (2002) Identification of a tyrosine in the agonist binding site of the homomeric $\rho 1$ γ -aminobutyric acid (GABA) receptor that, when mutated, produces spontaneous opening. *J. Biol. Chem.* **277**, 43741–43748
51. Taly, A., Corringer, P. J., Grutter, T., Prado de Carvalho, L., Karplus, M., and Changeux, J. P. (2006) Implications of the quaternary twist allosteric model for the physiology and pathology of nicotinic acetylcholine receptors. *Proc. Natl. Acad. Sci. U.S.A.* **103**, 16965–16970
52. Goldschen-Ohm, M. P., Wagner, D. A., Petrou, S., and Jones, M. V. (2010) An epilepsy-related region in the GABA_A receptor mediates long-distance effects on GABA and benzodiazepine binding sites. *Mol. Pharmacol.* **77**, 35–45
53. Miller, P. S., and Smart, T. G. (2010) Binding, activation and modulation of Cys-loop receptors. *Trends Pharmacol. Sci.* **31**, 161–174
54. Everitt, A. B., Seymour, V. A., Curmi, J., Laver, D. R., Gage, P. W., and Tierney, M. L. (2009) Protein interactions involving the $\gamma 2$ large cytoplasmic loop of GABA_A receptors modulate conductance. *FASEB J.* **23**, 4361–4369
55. Roy, S., Roy, S. J., Pinard, S., Taillefer, L. D., Rached, M., Parent, J. L., and Gallo-Payet, N. (2011) Mechanisms of melanocortin-2 receptor (MC2R) internalization and recycling in human embryonic kidney (hek) cells. Identification of key Ser/Thr (S/T) amino acids. *Mol. Endocrinol.* **25**, 1961–1977
56. Stein, B. S., Bensch, K. G., and Sussman, H. H. (1984) Complete inhibition of transferrin recycling by monensin in K562 cells. *J. Biol. Chem.* **259**, 14762–14772
57. Charych, E. I., Liu, F., Moss, S. J., and Brandon, N. J. (2009) GABA_A receptors and their associated proteins. Implications in the etiology and treatment of schizophrenia and related disorders. *Neuropharmacology* **57**, 481–495
58. Uusi-Oukari, M., and Korpi, E. R. (2010) Regulation of GABA_A receptor subunit expression by pharmacological agents. *Pharmacol. Rev.* **62**, 97–135
59. Tan, K. R., Brown, M., Labouèbe, G., Yvon, C., Creton, C., Fritschy, J. M., Rudolph, U., and Lüscher, C. (2010) Neural bases for addictive properties of benzodiazepines. *Nature* **463**, 769–774
60. Knabl, J., Witschi, R., Hösl, K., Reinold, H., Zeilhofer, U. B., Ahmadi, S., Brockhaus, J., Sergejeva, M., Hess, A., Brune, K., Fritschy, J. M., Rudolph, U., Möhler, H., and Zeilhofer, H. U. (2008) Reversal of pathological pain through specific spinal GABA_A receptor subtypes. *Nature* **451**, 330–334
61. Bouthour, W., Leroy, F., Emmanuelli, C., Carnaud, M., Dahan, M., Poncer, J. C., and Lévi, S. (2012) A Human Mutation in Gabrg2 Associated with Generalized Epilepsy Alters the Membrane Dynamics of GABA_A Receptors. *Cereb Cortex* **22**, 1542–1553
62. Krishek, B. J., Moss, S. J., and Smart, T. G. (1996) A functional comparison of the antagonists bicuculline and picrotoxin at recombinant GABA_A receptors. *Neuropharmacology* **35**, 1289–1298
63. Changeux, J. P., and Taly, A. (2008) Nicotinic receptors, allosteric proteins and medicine. *Trends Mol. Med.* **14**, 93–102
64. Sine, S. M., and Engel, A. G. (2006) Recent advances in Cys-loop receptor structure and function. *Nature* **440**, 448–455
65. Tierney, M. L. (2011) Insights into the biophysical properties of GABA_A ion channels. Modulation of ion permeation by drugs and protein interactions. *Biochim. Biophys. Acta* **1808**, 667–673
66. Peters, J. A., Cooper, M. A., Carland, J. E., Livesey, M. R., Hales, T. G., and Lambert, J. J. (2010) Novel structural determinants of single channel conductance and ion selectivity in 5-hydroxytryptamine type 3 and nicotinic acetylcholine receptors. *J. Physiol.* **588**, 587–596
67. Tsetlin, V., Kuzmin, D., and Kasheverov, I. (2011) Assembly of nicotinic and other Cys-loop receptors. *J. Neurochem.* **116**, 734–741
68. Chen, G., Kittler, J. T., Moss, S. J., and Yan, Z. (2006) Dopamine D3 receptors regulate GABA_A receptor function through a phospho-dependent endocytosis mechanism in nucleus accumbens. *J. Neurosci.* **26**, 2513–2521
69. Kittler, J. T., Chen, G., Kukhtina, V., Vahedi-Faridi, A., Gu, Z., Tretter, V., Smith, K. R., McAinsh, K., Arancibia-Carcamo, I. L., Saenger, W., Haucke, V., Yan, Z., and Moss, S. J. (2008) Regulation of synaptic inhibition by phospho-dependent binding of the AP2 complex to a YECL motif in the GABA_A receptor $\gamma 2$ subunit. *Proc. Natl. Acad. Sci. U.S.A.* **105**, 3616–3621
70. Gonzalez, C., Moss, S. J., and Olsen, R. W. (2012) Ethanol promotes clathrin adaptor-mediated endocytosis via the intracellular domain of δ -containing GABA_A receptors. *J. Neurosci.* **32**, 17874–17881
71. Liang, J., Suryanarayanan, A., Abriam, A., Snyder, B., Olsen, R. W., and Spigelman, I. (2007) Mechanisms of reversible GABA_A receptor plasticity after ethanol intoxication. *J. Neurosci.* **27**, 12367–12377
72. Saliba, R. S., Kretschmannova, K., and Moss, S. J. (2012) Activity-dependent phosphorylation of GABA_A receptors regulates receptor insertion and tonic current. *EMBO J.* **31**, 2937–2951

73. Jacob, T. C., Michels, G., Silayeva, L., Haydon, J., Succol, F., and Moss, S. J. (2012) Benzodiazepine treatment induces subtype-specific changes in $GABA_A$ receptor trafficking and decreases synaptic inhibition. *Proc. Natl. Acad. Sci. U.S.A.* **109**, 18595–18600
74. Bradley, C. A., Taghibiglou, C., Collingridge, G. L., and Wang, Y. T. (2008) Mechanisms involved in the reduction of $GABA_A$ receptor $\alpha 1$ -subunit expression caused by the epilepsy mutation A322D in the trafficking-competent receptor. *J. Biol. Chem.* **283**, 22043–22050
75. Ding, L., Feng, H. J., Macdonald, R. L., Botzolakis, E. J., Hu, N., and Gallagher, M. J. (2010) $GABA_A$ receptor $\alpha 1$ subunit mutation A322D associated with autosomal dominant juvenile myoclonic epilepsy reduces the expression and alters the composition of wild type $GABA_A$ receptors. *J. Biol. Chem.* **285**, 26390–26405
76. Macdonald, R. L., Kang, J. Q., and Gallagher, M. J. (2010) Mutations in $GABA_A$ receptor subunits associated with genetic epilepsies. *J. Physiol.* **588**, 1861–1869
77. DeLano, W. L. (2010) *The PyMOL Molecular Graphics System*, version 1.3r1, Schrodinger, LLC, New York